ELSEVIER

Chemical Geology 198 (2003) 21–31

CHEMICAL GEOLOGY
INCLUDING
ISOTOPE GEOSCIENCE

www.elsevier.com/locate/chemgeo

Ammonium quantification in muscovite by infrared spectroscopy

Vincent Busigny[a,*], Pierre Cartigny[a], Pascal Philippot[b], Marc Javoy[a]

[a] *Laboratoire de Géochimie des Isotopes Stables, UMR 7047, IPGP et Université Paris VII, 2 place Jussieu, 75252 Paris Cedex 05, France*
[b] *Laboratoire de Géosciences Marines, CNRS-FRE 2316, IPGP et Universités Paris VI et VII, 2 place Jussieu, 75252 Paris Cedex 05, France*

Received 23 May 2002; accepted 11 November 2002

Abstract

Single muscovite grains of different chemical composition (in particular Si-content from 3.05 to 3.69 per formulae unit (pfu)) and origin (metamorphic and granitic rocks) were analysed by infrared (IR) spectroscopy. Their ammonium concentrations were subsequently measured by capacitance manometry after extraction as N_2 using a sealed-tube combustion technique. The values range from 0 to 2203 ppm NH_4^+. Correlation between ammonium concentration and ammonium IR absorbance corresponding to NH_4^+ bending permits an assessment of the ammonium molecular absorptivity at 1430 cm^{-1} ($\varepsilon_{N-H}^{1430} = 462 \pm 32$ l mol^{-1} cm^{-1}). In order to avoid uncertainties on thickness estimates using an optical technique, a relationship between sample thickness and IR absorbance was determined. Ammonium concentration of muscovite can be directly derived from its IR spectrum using the relationship $[NH_4^+]$ (ppm) $= 1142.5 \times [(A_{N-H}^{1430} - A^{2514})/(A^{1282} - A^{2514})] - 606$ where A^{1282}, A_{N-H}^{1430} and A^{2514} are absorbances corresponding to wavenumbers 1282 (Si–O vibration peak), 1430 (NH_4^+ bending) and 2514 cm^{-1} (silicate network vibration), respectively. The precision of ammonium concentration estimates using this method is better than 20% (2σ) for muscovites thicker than 30 μm. This is independent of mineral composition, thus implying that the ammonium concentration vs. IR absorbance relationship is independent of the muscovite–celadonite solid solution.

Keywords: Infrared spectroscopy; Ammonium; Muscovite; Phengite

1. Introduction

Nitrogen has been shown to be a very powerful tracer in different geochemical systems. Milovskiy and Volynets (1966) and Urano (1971) suggested the use of nitrogen content as an indicator of the origin of metamorphic and granitic rocks. Ader et al. (1998) showed that the nitrogen isotopic signature of organic material is preserved during diagenesis processes, thus indicating that it can be used as a tool for reconstructing paleoecological and paleodepositional history. Williams et al. (1992) used the geochemical behavior of fixed nitrogen during diagenetic processes to trace hydrocarbon production and migration. Nitrogen content coupled with nitrogen isotope system has also been demonstrated as an effective tracer of devolatilization and fluid–rock interactions attending metamorphism (Duit et al., 1986; Haendel et al., 1986; Bebout and Fogel, 1992; Bebout, 1997; Mingram and Braüer, 2001).

* Corresponding author. Fax: +33-1-44-27-28-30.
E-mail address: busigny@ipgp.jussieu.fr (V. Busigny).

0009-2541/02/$ - see front matter © 2002 Elsevier Science B.V. All rights reserved.
doi:10.1016/S0009-2541(02)00420-5

Constraining the nitrogen exchange between mantle and exosphere requires a good knowledge of the amount of nitrogen degassed from the mantle and recycled via subduction zones. To date, few studies were devoted to the amount and isotopic composition of nitrogen in subducted metamorphic rocks (Haendel et al., 1986; Bebout and Fogel, 1992; Mingram and Braüer, 2001). Because of the earlier presence of organic matter in sediments, the major contribution of recycled nitrogen is certainly brought by pelites rather than mafic and ultramafic rocks. In metapelites, nitrogen occurs mainly as ammonium ion (NH_4^+), which is substituted for potassium in phengitic muscovites. Because several phengite generations exist in the same rock sample, prograde minerals have to be distinguished from retrograde minerals. Solving this problem requires both a detailed petrological analysis and a high-resolution ammonium quantification technique.

Conventional methods for the determination of ammonium concentration in rocks or minerals are based either on the decomposition of samples in acid solutions (Stevenson, 1959, 1962; Milovskiy and Volynets, 1966; Urano, 1971; Honma and Itihara, 1981; Williams et al., 1989, 1992; Williams and Ferrell, 1991; Mingram and Braüer, 2001) or on combustion or pyrolysis techniques under vacuum (Kendall and Grim, 1990; Bebout and Fogel, 1992; Bebout, 1997; Boyd et al., 1994; Boyd, 1997; Boyd and Philippot, 1998). For a single mineral like muscovite, N-content can be determined using Fourier Transform Infrared (FTIR) spectroscopy. Several infrared absorption studies have dealt with ammonium in micas (Vedder, 1964, 1965; Yamamoto and Nakahira, 1966; Karyakin et al., 1973; Higashi, 1978) but quantification based on this technique is poorly developed owing to a lack of knowledge of ammonium molecular absorptivity (ε_{N-H}). However, experimental techniques for determining ε_{N-H} are available (Boyd, 1997).

The present paper provides a calibration of the Beer–Lambert law applied to ammonium in muscovite. Adopting the method described by Agrinier and Jendrzejewski (2000), a correlation between muscovite thickness and infrared (IR) absorbance provides an empirical law for thickness spectroscopic measurements. Vacuum extraction and manometry were used to measure the N-content of spectroscopically characterised muscovites. Results allowed estimating ammonium molecular absorptivity of muscovite. Finally, the Beer–Lambert law is adapted to determine ammonium concentration directly from IR analysis.

2. Samples description and selection

In the present study, several types of single white mica grains were selected, including both muscovites ($n=47$) from granites and phengites ($n=89$) from metapelites. Table 1 provides a description of all samples analysed here, including the rock types from which muscovites were extracted (leucogranite, micaschist, calc-schist and quartzite), together with the location of the samples and the mineralogical assemblage of the rock. Grain size ranged between 2 and 10 mm. The mass of muscovite was comprised between 0.064 and 0.542 mg, that of phengite between 0.033 and 2.784 mg.

All mica compositions are part of the solid solution between muscovite end-member $KAl_2Si_3AlO_{10}(OH)_2$

Table 1
Rock types from which muscovites have been extracted, location of the samples and mineralogical assemblages of the rocks

Sample	Rock type	Location	Lithological context
LEUCO (muscovites)	leucogranite	Ploemeur (Armorican massif, NW France)	quartz + albite + orthoclase + biotite + muscovite
98SE8 (phengites)	HP calc–schist	Finestre's col (Schistes Lustrés, Western Italian Alps)	(garnet + phengite + chlorite + chloritoide) in a (quartz + carbonate) matrix
SL98-3C (phengites)	HP calc–schist	Assieta's col (Schistes Lustrés, Western Italian Alps)	(phengite + chlorite + biotite + graphite) in a (quartz + carbonate) matrix
80-3 and 59-4 (phengites)	HP mica–schist	Trescolmen (Central Alps, Switzerland)	(garnet + phengite + rutile + apatite + zircon) in a quartz matrix
DAB (phengites)	quartzite	Dabieshan massif (China)	quartz (coesite) + phengite
90-25B (phengites)	HP calc–schist	Lago di Cignana (Schistes Lustrés, Western Italian Alps)	(garnet + phengite + chlorite + zoisite ± biotite ± chloritoide ± rutile) in a (quartz(coesite) + carbonate) matrix

and celadonite end-member $K(Mg, Fe)AlSi_4O_{10}(OH)_2$. Many studies have shown that the celadonite content of muscovite increases with pressure (e.g. Velde, 1965, 1967; Schmidt, 1996; Domanik and Holloway, 2000) and decreases with increasing temperature (e.g. Velde, 1965; Guidotti and Sassi, 1976). Thus, phengite shows variable chemical compositions depending on the tschermak exchange Al^{VI}, $Al^{IV} \leftrightarrow (Mg, Fe^{2+})^{VI}$, Si^{IV}. Different populations of micas equilibrated at different $P-T$ conditions were analysed in this study. This allows testing the effect of mica chemical composition on the calibration procedure.

Samples were selected in the following way: (i) Sample purity: using a reflection and transmission binocular microscope, we rejected inclusion-bearing samples and those containing a darker (typical of biotite) or green (chlorite) colour. (ii) Sample thickness: sample thickness has been restricted from 20 to 600 μm due to handling problem and sensitivity threshold of the detector. Micas of 50 to 150 μm thickness produced the best results. (iii) Constant sample thickness: in order to avoid diffraction process of the IR light and to allow accurate thickness estimates, IR spectrometry quantification has been performed on samples with homogeneous and parallel faces.

3. Analytical techniques

Infrared measurements were carried out on single grains using a Fourier Transform Infrared (FTIR) spectrometer (Magna 550, Nicolet) coupled with an optical/IR microscope. An ''Ever-Glo'' (Nicolet) infrared source, a Ge over KBr beam splitter and a MCTA detector were used. Conditions of spectra acquisition include a resolution of 4 cm^{-1}, a mirror velocity of 3.16 cm s^{-1} and a scan number of 500. The beam size was approximately of 100 μm. Measurements of absorption bands' integrated intensity were made using the OMNIC software supplied with the Nicolet instrument. The use of IR spectroscopy for quantitative analysis requires good control of mineral orientation. All analyses were performed with an IR beam direction perpendicular to the ⟨001⟩ crystallographic direction (i.e. to the layer). We also attempted to do it parallel to ⟨001⟩. However, beam focusing was characterised by a strong diffraction.

Major element contents of muscovite were determined using an electron microprobe (CAMEBAX, University Paris VI). The acceleration voltage was 15 kV and the sample current was 10 nA. The counting times were 40 s for fluorine and 10 s for all other elements. The spot size was 10 μm.

Nitrogen quantification was performed using a sealed-tube combustion technique with CuO, Cu and CaO in order to trap both CO_2 and H_2O (Kendall and Grim, 1990; Boyd and Pillinger, 1990; Boyd et al., 1994, 1995; Ader, 1999). The experimental protocol followed in this study was described by Boyd (1997). However, a combustion was preferred rather than pyrolysis as it gives more reproducible results for low N quantities (≈ 10 nmol; Ader, 1999). A summary of the technique used for nitrogen extraction is given below.

CuO, Cu and CaO were loaded in quartz glass tubes and degassed at 700 °C for 24 h on a vacuum line. The tubes were then sealed under vacuum and heated in a muffle furnace at 950 °C for 6 h followed by a step at 600 °C for 2 h in order to purify the reactants. The tubes were again attached to the preparation line and heated at 700 °C. After 10 min, the line was evacuated to pressure lower than 10^{-6} Torr. Temperature was reduced to 450 °C and samples (single grains weighing between 0.033 and 2.784 mg) were dropped on the top of the reactants (Boyd and Pillinger, 1990). The tubes were isolated from the pumps and the line was saturated with O_2 pressure generated with CuO heated to 900 °C for 1 h. This step allows removing all organic contamination and adsorbed atmospheric nitrogen, if any. O_2 was then readsorbed by cooling the CuO to 450 °C and the line was evacuated. At pressure lower than 10^{-6} Torr, the tubes were sealed to give evacuated ampoules. Those ampoules were heated in a muffle furnace at 950 °C for 6 h and 600 °C for 2 h for the following reasons: (i) sample combustion under oxygen pressure at 950 °C, (ii) nitrous oxide reduction by copper and (iii) trapping of carbon dioxide by CaO at 600 °C. The tubes were then slowly cooled to room temperature allowing water to react with CaO. Ampoules were loaded into a vacuum line and opened with a tube cracker. Combustion gases were transferred using a molecular sieve cooled to liquid nitrogen temperature. Nitrogen was purified and quantified as dinitrogen N_2 by capacitance manometry with a precision better than

8% (2σ). This precision was determined from the replicated analysis of several homogeneous powders. Each series of analysis contained four analyses including three samples and one blank so that each sample was blank-corrected. The reason for measuring one blank each time arises from the variability of nitrogen amount in blanks ranging from 0.1 to 2 nmol (mean value = 0.5 nmol).

4. Principles of quantification by infrared spectroscopy

4.1. White mica IR spectroscopy

A typical muscovite infrared absorption spectrum is shown in Fig. 1. Each absorption band corresponds to a specific vibration of molecular units in the crystal (Vedder, 1964, 1965; Karyakin et al., 1973; Farmer, 1974; Higashi, 1978). The mid-IR spectral range comprises (i) intense absorption in the 3620–3630 cm^{-1} region caused by vibrations of hydroxyl groups, (ii) the two N–H bound vibrations at 1430 cm^{-1} (N–H bending) and from 2800 to 3400 cm^{-1} (N–H stretching), and (iii) Si–O stretching vibrations lying in the 700–1200 cm^{-1} region. Combination bands involving the O–H stretching mode and some other lower frequency modes occur in a range from 1730 to 2150 cm^{-1} (Vedder, 1964).

4.2. The Beer–Lambert law

The Beer–Lambert law predicts a proportional relationship between molecular species absorbance and concentration in the sample. For a given wave number μ, the Beer–Lambert law is of the form,

$$A_X^{\mu} = \frac{d\rho\varepsilon_X^{\mu}}{M_X}[X] \quad (1)$$

where A_X^{μ} is the absorbance of the molecular species X (logarithmic unit) at a wavenumber μ, ρ and d the density (g cm^{-3}) and the thickness (cm) of the sample, respectively, $[X]$ the concentration (ppm by weight) of the species X in the analysed mineral, ε_X^{μ} the molecular absorptivity (l mol^{-1} cm^{-1}) of the molecular species X at the wavenumber μ and M_X its molecular weight (mg mol^{-1}). Assessing the concentration of the molecular species X by IR spectrometry requires a good knowledge of the density, the thickness and the molecular absorptivity of the species X under consideration.

Muscovite and celadonite densities are about 2.8 and 3.0 g cm^{-3} (Nickel and Nichols, 1991), respectively. We used a constant density value of 2.9 ($\pm$ 0.1) g cm^{-3} herein.

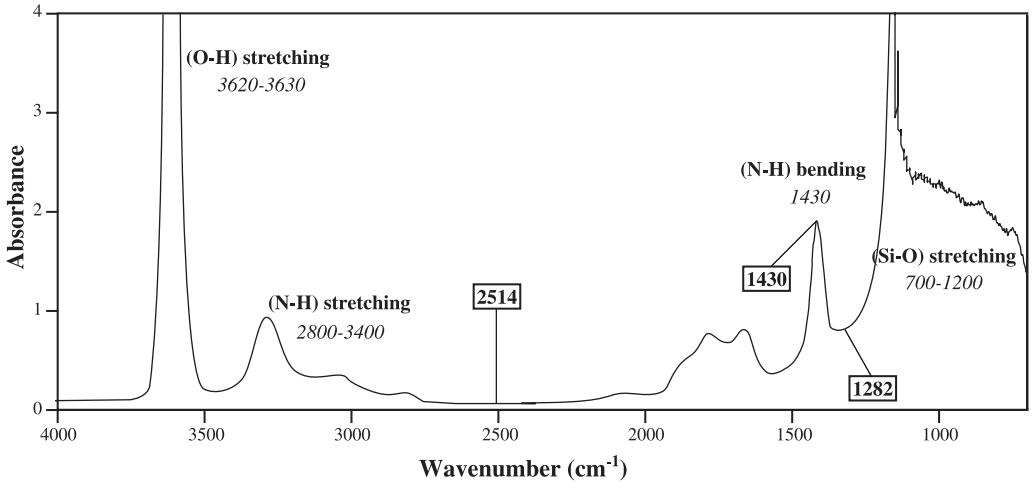

Fig. 1. Infrared spectrum of a phengitic muscovite from the western Alps (sample 98SE8). Each vibration band is associated to a molecular bound (bold) and a frequency domain (italic). Sample thickness is 107 μm ($\pm$ 10 μm).

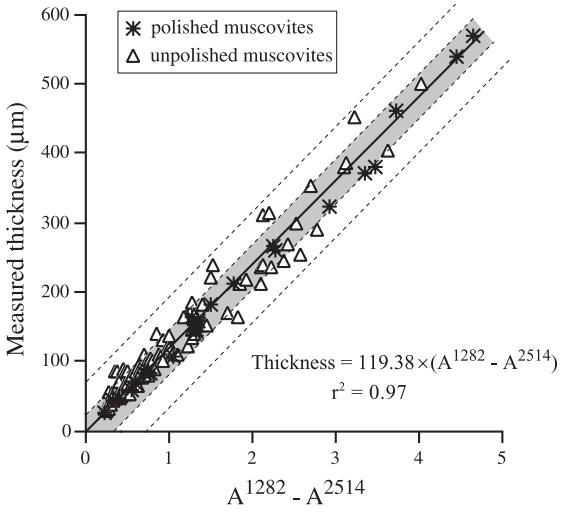

Fig. 2. Linear relationship observed between sample thickness and difference of IR absorbances ($A^{1282} - A^{2514}$) for muscovites. Dark and clear areas represent, respectively, polished (stars) and unpolished (triangles) muscovites.

Sample thickness was measured with a digital micrometer with a precision of ± 1 µm. The thickness of a sample is measured after the IR spectrum is obtained and required the sample to be transferred from the IR spectrometer to a micrometer. This may be a source of inaccuracy if thickness and IR measurements are not performed exactly at the same location.

4.3. Direct measurement of thickness from silicate network absorption

We tested the method applied by Agrinier and Jendrzejewski (2000) in which sample thickness is deduced directly from IR spectrum. The Beer–Lambert law predicts a proportionality relationship between sample thickness and IR light absorbance. If one applies the Beer–Lambert law (Eq. (1)) to molecular species X for a wavenumber μ, one can write for samples 1 and 2:

$$\frac{(A_X^{\mu})_1}{(A_X^{\mu})_2} = \frac{d_1\rho_1(\varepsilon_X^{\mu})_1[X_1]}{d_2\rho_2(\varepsilon_X^{\mu})_2[X_2]} \quad (2)$$

Given that samples 1 and 2 are dioctaedral micas, their densities are considered equal (i.e. $\rho_1 = \rho_2$). Assuming that X is a major molecular species (for example SiO_4^{4-}), its concentration is similar in the two samples analysed (i.e. $[X_1]=[X_2]$). Accordingly, $(\rho_1(\varepsilon_X^{\mu})_1[X_1])/(\rho_2(\varepsilon_X^{\mu})_2[X_2]) = 1$ and Eq. (2) reduces to

$$\frac{(A_X^{\mu})_1}{(A_X^{\mu})_2} = \frac{d_1}{d_2} \quad (3)$$

Eq. (3) states that, for a given mineral, the absorbance of major molecular species is directly proportional to sample thickness.

In order to avoid error linked with baseline correction, we used an absorbance difference between two absorbances due to silicate network rather than an absolute absorbance. The relationship between sample thickness and the silicate network was checked over the full range of wave numbers (i.e. 1230–1340 and 2250–2650 cm^{-1}). The specific wave numbers of each absorbance were determined randomly so as to obtain the best possible thickness/absorbance correla-

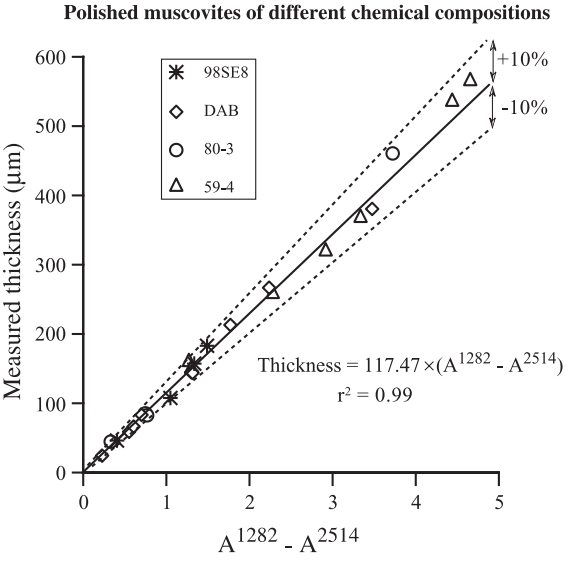

Fig. 3. Linear relationship between sample thickness and IR light absorbance differences ($A^{1282} - A^{2514}$) for polished muscovites. Symbols correspond to muscovites from: HP metapelites 98SE8 (stars), 80-3 (circles) and 59-4 (triangles) and UHP quartzite DAB (rhombus). Best-fit line equation allows an assessment of muscovite thickness directly by the used of IR light absorbances A^{1282} and A^{2514}. The two dashed lines represent a deviation to the mean line of ± 10%.

tion. It was found that the absorbance difference between 1282 and 2514 cm^{-1} provides the best results (Fig. 2). The first absorbance at 1282 cm^{-1} is located on a side of Si–O vibration peak and the second at 2514 cm^{-1} corresponds to silicate network vibration (Fig. 1). Thickness estimates were performed on polished and unpolished muscovites, ranging from 24 to 568 and 27 to 499 μm, respectively. They are plotted as a function of the absorbance difference between 1282 and 2514 cm^{-1} in Fig. 2. Data display a general linear trend including the two-muscovite populations. According to the Beer–Lambert law, absorbance must be zero when thickness is zero. Data can be fitted using the "passing through origin" condition:

$$d_{\text{muscovite}}(\mu m) = 119.38 \times (A^{1282} - A^{2514}) \quad r^2 = 0.97 \tag{4}$$

where $d_{\text{muscovite}}$ is the muscovite thickness and A^{1282} and A^{2514} the absorbance for wavenumbers 1282 and 2514 cm^{-1}. Because data scattering is larger for unpolished samples (clear area) than for polished samples (dark area), a linear relationship determined solely from polished samples (see Fig. 3) was preferred:

$$d_{\text{muscovite}}(\mu m) = 117.47 \times (A^{1282} - A^{2514}) \quad r^2 = 0.99 \tag{5}$$

the precision on the thickness measurement being better than ± 10% (2σ; Fig. 3).

A further potential problem may be linked to muscovite chemistry. Table 2 reports the chemical composition of the different muscovites analysed in this study. Major element composition is given in wt.% for oxides and in per formulae unit (pfu) calculated on the basis of 11 oxygens. Table 2 shows that muscovite Si-content varies from 3.05 pfu for granite muscovite (LEUCO) to 3.69 pfu for metapelite phengite (98SE8). Al-content varies from 2.76 (LEUCO) to 1.64 pfu (98SE8). (Fe + Mg) content range between 0.17 and 0.68 pfu, and correlate positively with Si-content as a result of the tschermak substitution. Polished samples (98SE8, DAB, 80-3 and 59-4) show a wide range of compositions with Si-content varying from 3.41 to

Table 2
Muscovites chemical composition in major elements (oxides in wt.%, formulae in pfu are calculated on the basis of 11 oxygens)

Sample	98SE8	DAB	80-3	59-4	90-25B	SL98-3C	LEUCO
SiO_2	55.60	53.04	52.93	51.20	50.74	50.33	45.70
TiO_2	0.07	0.31	0.46	0.39	0.20	0.10	1.09
Al_2O_3	21.03	24.44	26.49	27.44	28.69	28.80	35.15
FeO (t)	4.48	2.05	1.52	1.96	2.17	3.22	1.79
MnO	0.05	0.00	0.16	0.00	0.03	0.00	0.00
MgO	4.42	4.36	4.21	3.37	3.00	2.18	0.74
CaO	0.00	0.00	0.01	0.05	0.00	0.17	0.00
Na_2O	0.04	0.23	0.40	0.54	0.59	0.22	0.58
K_2O	11.01	11.23	10.36	10.17	9.90	10.22	10.21
F	0.21	0.00	0.14	0.00	0.25	0.00	0.13
Total	96.89	95.65	96.67	95.11	95.56	95.23	95.39
Si	3.69	3.53	3.46	3.41	3.37	3.36	3.05
Ti	0.00	0.02	0.02	0.02	0.01	0.00	0.05
Al	1.64	1.92	2.04	2.15	2.24	2.27	2.76
Fe	0.25	0.11	0.08	0.11	0.12	0.18	0.10
Mn	0.00	0.00	0.01	0.00	0.00	0.00	0.00
Mg	0.44	0.43	0.41	0.33	0.30	0.22	0.07
Ca	0.00	0.00	0.00	0.00	0.00	0.01	0.00
Na	0.00	0.03	0.05	0.07	0.08	0.03	0.07
K	0.93	0.95	0.86	0.86	0.84	0.87	0.87
F	0.04	0.00	0.03	0.00	0.05	0.00	0.03

3.69 pfu. Such compositional variations may have an influence on 1282 and 2514 cm^{-1} absorbances. Fig. 3 shows that polished muscovites display a relatively good correlation in terms of mineral thickness vs. absorbance, implying that the influence of chemical composition is negligible. Accordingly, the relation (Eq. (5)) between thickness and $A^{1282} - A^{2514}$ seems applicable to muscovites as a whole, independent of their chemical composition.

5. Calibration

According to the Beer–Lambert law (Eq. (1)), the plot of ammonium concentration as a function of ammonium absorbance/muscovite thickness ratio must vary linearly. Several standard methods for deriving ammonium absorbance (A^{μ}_{N-H}) from heights and areas of nitrogen vibration peaks consist in substituting for A^{μ}_{N-H}: (i) area of ammonium bending (1430 cm^{-1}) and stretching (from 2750 to 3480 cm^{-1}) vibration peaks corrected by a straight baseline; (ii) maximum height of ammonium bending (1430 cm^{-1}) and stretching (from 2750 to 3480 cm^{-1}) vibration peaks calculated for a straight baseline; (iii) area of ammonium bending from which the spectrum of a very low N-content phengite is subtracted. This subtraction allows in theory to distinguish the respective absorbances of ammonium and silicate network.

Because three absorption bands are superimposed in the region 1100–1700 cm^{-1} (i.e. Si–O stretching, N–H bending and the network vibration peak at 1680 cm^{-1}), baseline was difficult to choose and the best results arise from the use of an absorbance difference between maximum height of ammonium peak at 1430 cm^{-1} (± 5 cm^{-1}) and the silicate network vibration at 2514 cm^{-1} (see Fig. 1).

Nitrogen contents were determined for 33 white micas, including 26 metapelitic phengites (90-25B, 98SE8, DAB, 80-3, 59-4 and SL98-3C) and 7 granitic muscovites (LEUCO). Table 3 summarises sample weight, sample thickness calculated using Eq. (5), ammonium absorbance/thickness ratio and ammonium content determined from sealed-tube extraction technique. Ammonium content varies from 0 to 2203 ppm in phengite and from 307 to 426 ppm in muscovite from leucogranite. Sample thicknesses and weights are comprised between 30 and 396 μm, and 0.033 and 2.784 mg, respectively. Ammonium content is shown as a function of ammonium absorbance/thickness ratio in Fig. 4. Each point corresponds to a single muscovite grain. Because of the possible grain inhomogeneity, ammonium absorbance/thick-

Table 3
Sample weight (mg), calculated thickness (μm), ammonium absorbance/thickness ratio (cm^{-1}) and ammonium content (ppm) of 26 metapelitic phengites (90-25B, 98SE8, DAB, 80-3, 59-4 and SL98-3C) and 7 granitic muscovites (LEUCO)

Sample	Weight (mg)	Calculated thickness (μm)	$(A^{1430}_{N-H} - A^{2514})$/ thickness ($cm^{-1}$)	$[NH_4^+]$ (ppm)
90-25B#1	0.058	50	184	1684 ($\pm$ 136)
90-25B#2	0.034	60	182	1522 ($\pm$ 127)
90-25B#3	0.182	101	153	1584 ($\pm$ 124)
90-25B#4	0.061	73	156	1599 ($\pm$ 120)
90-25B#5	0.063	34	175	1761 ($\pm$ 135)
90-25B#6	0.311	117	174	1763 ($\pm$ 139)
90-25B#7	0.140	54	183	1745 ($\pm$ 136)
98SE8#1	0.597	396	149	1619 ($\pm$ 129)
98SE8#2	1.039	144	183	2099 ($\pm$ 170)
98SE8#3	0.330	233	166	1814 ($\pm$ 144)
98SE8#4	0.183	175	205	2080 ($\pm$ 172)
98SE8#5	0.033	40	174	1522 ($\pm$ 127)
98SE8#6	0.390	90	181	2203 ($\pm$ 175)
98SE8#7	0.278	99	193	1845 ($\pm$ 146)
98SE8#8	0.109	65	181	1671 ($\pm$ 130)
98SE8#9	0.119	51	186	1845 ($\pm$ 145)
98SE8#10	0.160	103	151	1812 ($\pm$ 143)
98SE8#11	0.092	36	188	1846 ($\pm$ 145)
SL98-3C#1	0.035	66	114	865 ($\pm$ 70)
SL98-3C#2	0.040	91	122	940 ($\pm$ 76)
DAB#1	0.487	47	47	56 ($\pm$ 6)
DAB#2	0.488	49	49	0 (–)
DAB#3	1.533	46	46	19 ($\pm$ 1)
80-3#1	2.784	52	52	108 ($\pm$ 8)
80-3#2	1.103	53	53	74 ($\pm$ 5)
59-4#1	0.316	57	57	151 ($\pm$ 15)
LEUCO#1	0.460	68	78	399 ($\pm$ 32)
LEUCO#2	0.542	81	73	372 ($\pm$ 30)
LEUCO#3	0.204	47	70	317 ($\pm$ 25)
LEUCO#4	0.134	30	73	426 ($\pm$ 30)
LEUCO#5	0.259	43	65	307 ($\pm$ 23)
LEUCO#6	0.064	55	79	384 ($\pm$ 23)
LEUCO#7	0.384	79	76	319 ($\pm$ 24)

Sample weight accuracy is better than 10^{-3} mg. Sample thickness was calculated from IR spectra using the relationship "$d_{muscovite} = 117.47 \times (A^{1282} - A^{2514})$". Ammonium contents were determined by a sealed-tube extraction technique. Their uncertainties (values in parenthesis) vary between 8% and 11%.

ness ratio corresponds to a mean value of six IR analyses performed at different location in a same grain. As expected, ammonium concentration varies linearly with ammonium absorbance/thickness ratio. The relationship is of the form,

$$[NH_4^+]\ (\text{ppm}) = 13.4 \times \frac{A^{1430}_{N-H} - A^{2514}}{\text{thickness (cm)}} - 606$$

(see Fig. 4) where $[NH_4^+]$ is a function of thickness and of two IR absorbances: A^{1430}_{N-H} at 1430 cm^{-1} and A^{2514} at 2514 cm^{-1}. According to Eq. (5), ammonium concentration can subsequently be expressed in the following way,

$$[NH_4^+]\ (\text{ppm}) = 1142.5 \times \frac{A^{1430}_{N-H} - A^{2514}}{A^{1282} - A^{2514}} - 606 \quad (6)$$

where A^{1282} is the IR absorbance at 1282 cm^{-1}. Using this relation, ammonium concentration in muscovite can be directly determined by IR spectrometry.

An important observation is that the linear regression does not intersect the origin of the plot. This result

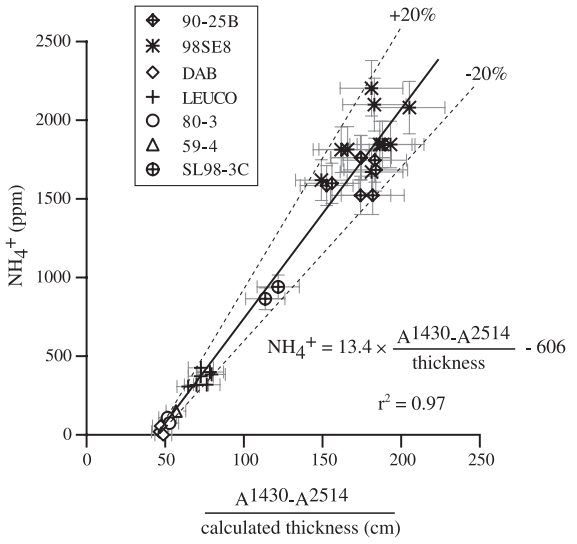

Fig. 4. Correlation between ammonium concentration (ppm) and ammonium absorbance/sample thickness ratio (cm^{-1}). From the line slope, ammonium molecular absorptivity coefficient at 1430 cm^{-1} can be deduced: a value of 462 ± 32 l mol cm^{-1} is found. The two dashed lines represent a deviation to the mean line of ± 20%.

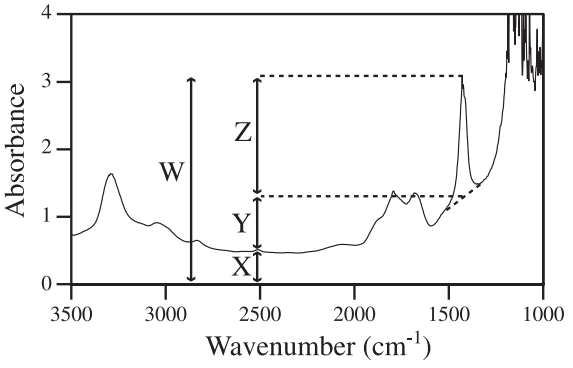

Fig. 5. Example of an infrared spectrum of a phengitic muscovite (sample 98SE8, from the Western Alps). It shows the definition of four absorbance values: *W*, *X*, *Y* and *Z*.

reflects the fact that an absorbance difference was used rather than a baseline-corrected absorbance for quantification. Qualitatively, the origin intersect corresponds to height difference between the baseline at 1430 cm^{-1} (N–H bending vibration) and the silicate network vibration at 2514 cm^{-1}. Quantitatively, the calibration is described below.

Fig. 5 shows the definition of four absorbance values (*W*, *X*, *Y* and *Z*) used in the present spectroscopic method. Absorbances *X* and *Y* are only functions of thickness (*d*) because they correspond to the silicate network vibration, thus $X = a \times d$ and $Y = b \times d$, where *a* and *b* are constants. Absorbance *W* can be expressed as $W = X + Y + Z$.

The Beer–Lambert law provides:

$$[NH_4^+] = \frac{M_{NH_4^+}}{d_{\text{muscovite}}\rho_{\text{muscovite}}\varepsilon^{\mu}_{N-H}} \times Z \quad (7)$$

(i.e.)

$$[NH_4^+] = \frac{M_{NH_4^+}}{d_{\text{muscovite}}\rho_{\text{muscovite}}\varepsilon^{\mu}_{N-H}} \times (W - X - Y) \quad (8)$$

(i.e.)

$$[NH_4^+] = \frac{M_{NH_4^+}}{d_{\text{muscovite}}\rho_{\text{muscovite}}\varepsilon^{\mu}_{N-H}} \times (W - X) - \frac{M_{NH_4^+} b}{\rho_{\text{muscovite}}\varepsilon^{\mu}_{N-H}} \quad (9)$$

In the present case, $W=A^{1430}_{N-H}$ and $X=A^{2514}$ thus yielding:

$$[NH_4^+] = \frac{M_{NH_4^+}}{\rho_{muscovite}\varepsilon^{1430}_{N-H}} \times \frac{(A^{1430}_{N-H} - A^{2514})}{d_{muscovite}} - \frac{M_{NH_4^+} b}{\rho_{muscovite}\varepsilon^{1430}_{N-H}} \quad (10)$$

Eq. (10) details the solution of the linear relationship found in Fig. 4. The second term (i.e. $(M_{NH_4^+} b)/(\rho_{muscovite}\varepsilon^{1430}_{N-H})$) is a constant which represents intersect at the origin. Accordingly, the slope of the linear correlation in Fig. 4 is of the form "$(M_{NH_4^+})/(\rho_{muscovite}\varepsilon^{1430}_{N-H})$". As the values for $M_{NH_4^+}$ and $\rho_{muscovite}$ are known, the best-fit slope allows determining ammonium molecular absorptivity at 1430 cm^{-1} (ε^{1430}_{N-H}). This assessment provides a value of 462 ± 32 l mol^{-1} cm^{-1}.

Although samples display a general linear correlation in Fig. 4, a slight scattering is observed. This scattering can be explained by several causes: (i) analytical precision on nitrogen extraction technique, (ii) precision on infrared analysis (as absorbance is a logarithmic value, the higher the absorbance, the worse the precision), and (iii) heterogeneity of ammonium concentration of the specimen. This later source of uncertainties was considered by calculating ammonium concentrations in each muscovite grain from infrared data. On average, calculated concentrations range between 300 and 400 ppm in granite muscovite and 1600 and 2000 ppm in metapelite phengite of high N-content. Thus, differences of N-content within a single mica are of the order of 20%, which cannot be neglected.

Several samples were analysed at the same location several times with different orientations (10 rotations of $\approx 40°$) around the perpendicular to ⟨001⟩ crystallographic direction. The standard deviations on the term "$A^{1430}_{N-H} - A^{2514}$" were found to be lower than 3%. It includes potential anisotropic effect and IR analytical error. The worse precision at highest absorbances may be caused by nonlinear detector behavior due to saturation effect. The precision on thickness spectroscopic measurement being about 10% (see above), the precision on the ammonium absorbance/thickness ratio is taken to be 11% in Fig. 4. Uncertainties on ammonium concentration measured by combustion technique are given in Table 3 (in parenthesis). They represent between 8% and 11% of the corresponding concentrations. A precision better than 20% (2σ; see Fig. 4) is expected when calculating ammonium concentrations by the method described herein. However, this precision can be worse than 50% for sample thickness lower than 30 μm. When the sample is very thin, very little absorption occurs and the difference between sample and background intensities is too low. The relative error becomes also large when the intensity of the N–H band is very low. Indeed, at low N-contents, large relative changes in the N–H band intensity will be associated with only small changes of $A^{1430}_{N-H} - A^{2514}$. This is especially due to the superimposed network vibrations in this wave number range.

6. Conclusion

In a range from 30 to 600 μm, muscovite thickness can be determined directly from FTIR spectra with a precision of 10%. Owing to crystal anisotropy, IR analyses have to be done with beam perpendicular to crystallographic direction ⟨001⟩.

An assessment of ammonium molecular absorptivity in muscovite for a wavenumber of 1430 cm^{-1} (N–H bending) gave a value of 462 ± 32 l mol^{-1} cm^{-1}. One can also express the Beer–Lambert law in a way that ammonium concentration in muscovite can be calculated from a function of IR absorbances A^{1282}, A^{1430}_{N-H} and A^{2514}. This method allows a quick and not destructive measurement of N-content in the sample with a precision better than 20%. Because of a possible ammonium concentration inhomogeneity, several analyses are necessary to obtain an average value in a single crystal. In other respect, this method could allow a study of the variability of ammonium concentration in a single grain or in several crystals of a single rock sample.

Acknowledgements

Thomas Zack, Serge Fourcade, Danièle Velde and Thomas Reinecke are gratefully acknowledged for providing rock samples. We would like to thank Pierre Agrinier, Jérôme Chmeleff, Cyril Aubaud and Svieta

Shilobreeva for their helpful comments. Michel Girard and Jean-Jacques Bourrand are thanked for their technical assistance. We would also like to thank Eddy Petit, Magali Ader, Isabelle Martinez and Nathalie Jendrzejewski for their advices about nitrogen extraction and FTIR techniques. Anonymous reviewers are thanked for their constructive comments. This paper is dedicated to Stuart Boyd, our colleague and friend, who left us last year. He inspired the present work through his "prelude" paper (Boyd, 1997). Contribution IPGP No. 1855 and CNRS No. 328. **[CA]**

References

Ader, M., 1999. Histoire isotopique de l'azote organique de la diagénèse au métamorphisme. PhD thesis, Université Paris 7, IPGP, France, pp. 144–181.

Ader, M., Boudou, J.P., Javoy, M., Goffé, B., Daniels, E., 1998. Isotope study on organic nitrogen of Westphalian anthracites from the Western Middle field of Pennsylvania (USA) and from the Bramsche Massif (Germany). Org. Geochem. 29, 315–323.

Agrinier, P., Jendrzejewski, N., 2000. Overcoming problems of density and thickness measurements in FTIR volatile determinations: a spectroscopic approach. Contrib. Mineral. Petrol. 139 (3), 265–272.

Bebout, G.E., 1997. Nitrogen isotope tracers of high-temperature fluid–rock interactions: case study of the Catalina Schist, California. Earth Planet. Sci. Lett. 151, 77–90.

Bebout, G.E., Fogel, M., 1992. Nitrogen-isotope compositions of metasedimentary rocks in the Catalina Schist, California: implications for metamorphic devolatilization history. Geochim. Cosmochim. Acta 56, 2839–2849.

Boyd, S.R., 1997. Determination of the ammonium content of potassic rocks and minerals by capacitance manometry: a prelude to the calibration of FTIR microscopes. Chem. Geol. 137, 57–66.

Boyd, S.R., Philippot, P., 1998. Precambrian ammonium biogeochemistry: a study of the Moine metasediments, Scotland. Chem. Geol. 144, 257–268.

Boyd, S.R., Pillinger, C.T., 1990. Determination of the abundance and isotope composition of nitrogen within organic compounds: a sealed tube technique for use with static vacuum mass spectrometers. Meas. Sci. Technol. 1, 1176–1183.

Boyd, S.R., Rejou-Michel, A., Javoy, M., 1994. Noncryogenic purification of nanomole quantities of nitrogen gas for isotopic analysis. Anal. Chem. 66, 1396–1402.

Boyd, S.R., Rejou-Michel, A., Javoy, M., 1995. Improved techniques for the extraction, purification and quantification of nanomole quantities of nitrogen gas: the nitrogen content of diamond. Meas. Sci. Technol. 6, 297–305.

Domanik, K.J., Holloway, J.R., 2000. Experimental synthesis and phase relations of phengitic muscovite from 6.5 to 11 GPa in a calcareous metapelite from the Dabie Mountains, China. Lithos 52, 51–77.

Duit, W., Jansen, J.B.H., Van Breemen, A., Bos, A., 1986. Ammonium micas in metamorphic rocks as exemplified by dome de l'Agout (France). Am. J. Sci. 286, 702–731.

Farmer, V.C., 1974. The layer silicates. In: Farmer, V.C. (Ed.), The Infrared Spectra of Minerals. Mineralogical Society, London, pp. 331–363.

Guidotti, C.V., Sassi, F.P., 1976. Muscovite as a petrogenetic indicator mineral in pelitic schists. Neues Jahrb. Mineral. Abh. 127, 97–142.

Haendel, D., Mühle, K., Nitzsche, H.M., Stiehl, G., Wand, U., 1986. Isotopic variations of the fixed nitrogen in metamorphic rocks. Geochim. Cosmochim. Acta 50, 749–758.

Higashi, S., 1978. Dioctaedral mica minerals with ammonium ions. Mineral. J. 9, 16–27.

Honma, H., Itihara, Y., 1981. Distribution of ammonium in minerals in metamorphic and granitic rocks. Geochim. Cosmochim. Acta 45, 983–988.

Karyakin, A.V., Volynets, V.F., Krieventsova, G.A., 1973. Investigation of nitrogen compounds in micas by infrared spectroscopy. Geochem. Int. 3, 326–329.

Kendall, C., Grim, E., 1990. Combustion tube method for measurement of nitrogen isotope ratios using calcium oxide for total removal of carbon dioxide and water. Anal. Chem. 62, 525–529.

Milovskiy, A.V., Volynets, V.F., 1966. Nitrogen in metamorphic rocks. Geochem. Int. 3, 752–758.

Mingram, B., Braüer, K., 2001. Ammonium concentration and nitrogen isotope composition in metasedimentary rocks from different tectonometamorphic units of the European Variscan Belt. Geochim. Cosmochim. Acta 65, 273–287.

Nickel, E.H., Nichols, M.C., 1991. Mineral Reference Manual. Van Nostrand-Reinhold, New York, pp. 36 and 143.

Schmidt, M.W., 1996. Experimental constraints on recycling of potassium from subducted oceanic crust. Science 272, 1927–1930.

Stevenson, F.J., 1959. On the presence of fixed ammonium in rocks. Science 130, 221–222.

Stevenson, F.J., 1962. Chemical state of nitrogen in rocks. Geochim. Cosmochim. Acta 26, 797–809.

Urano, H., 1971. Geochemical and petrological study on the origins of metamorphic rocks and granitic rocks by determination of fixed ammoniacal nitrogen. J. Earth Sci., Nagoya Univ. 19, 1–24.

Vedder, W., 1964. Correlations between infrared spectrum and chemical composition of mica. Am. Mineral. 49, 736–768.

Vedder, W., 1965. Ammonium in muscovite. Geochim. Cosmochim. Acta 29, 221–228.

Velde, B., 1965. Phengitic micas: synthesis, stability and natural occurrence. Am. J. Sci. 263, 886–913.

Velde, B., 1967. Si^{4+} content of natural phengites. Contrib. Mineral. Petrol. 14, 250–258.

Williams, L.B., Ferrell, R.E., 1991. Ammonium substitution in illite during maturation of organic matter. Clays Clay Miner. 39, 400–408.

Williams, L.B., Ferrell, R.E., Chinn, E.W., Sassen, R., 1989. Fixed ammonium in clays associated with crude oils. Appl. Geochem. 4, 605–616.

Williams, L.B., Wilcoxon, B.R., Ferrell, R.E., Sassen, R., 1992. Diagenesis of ammonium during hydrocarbon maturation and migration, Wilcox Group, Louisiana, USA. Appl. Geochem. 7, 123–134.

Yamamoto, T., Nakahira, M., 1966. Ammonium in sericites. Am. Mineral. 51, 1775–1787.